島根大学地球資源環境学研究報告　23, 39～48 ページ（2004 年 12 月）
Geoscience Rept. Shimane Univ., 23, p.39～48（2004）

Article

Major and trace element analyses of Miocene rocks from the Shinji–Matsue district and Shimane Peninsula, SW Japan

Barry Roser*, Rie Fujii* and Shinji Hashimoto*

Abstract

Major and trace element analyses of mainly sedimentary rocks from the Kawai-Kuri, Omori, Ushikiri, and Fujina Formations were made to add to a growing database for Miocene backarc sediments in Shimane, SW Japan. Samples were collected in the Shinji-Matsue district and in Shimane Peninsula. Kawai-Kuri sandstones and mudrocks are silica-rich, and most elements are depleted relative to Upper Continental Crust (UCC), suggesting derivation from a felsic granitoid source. Overlying Omori Formation volcanogenic sandstones have considerably lower SiO_2 contents and abundances of other elements lie closer to UCC, reflecting derivation from coeval Omori andesites and dacites. Deeper water turbiditic sediments in the correlative Ushikiri Formation have almost identical compositions. Mudrocks and very fine-grained sandstones from the Fujina Formation are moderately SiO_2-rich, and have elemental abundances similar to or less than UCC. This and immobile element ratios imply a mixed source comprising felsic granitoids and subordinate Omori volcanic and sedimentary rocks. The succession thus records initial exposure and erosion of basement granitoids, superimposed volcanism, and subsequent stripping of the volcanic cover.

Key words: Geochemistry, sandstone, mudstone, Miocene, Shimane

Introduction

Miocene sedimentary rocks crop out extensively in the San'in district of SW Japan in the area between the Chugoku mountains and the Japan Sea. Deposition occurred during and after opening of the Japan Sea, which began in Eocene - early Oligocene times (Takayasu *et al.,* 1992). The Miocene sediments are thus representative of back-arc deposition, during active rifting, subsidence of crustal blocks, and volcanism.

In the area around Izumo and Matsue, Miocene units crop out extensively in Shimane Peninsula, and also in a strip on the northern side of the Chugoku Mountains, on the south side of the topographic low occupied by the Izumo Plains and the Shinji-Nakaumi lake system (Fig. 1). The stratigraphy and depositional environments of these formations have been well studied (e.g. Kano *et al.,* 1991, 1994; Takayasu *et al.,* 1992), and their local correlations are well established.

Geochemical analyses of sedimentary rocks have become widely used in recent years to examine provenance signatures, tectonic setting, weathering/denudation histories, and other aspects of geology. Although many geochemical analyses of sedimentary rocks are now available in the literature, those from definite back arc settings are comparatively few. The San'in Miocene succession thus gives the opportunity to acquire data for sediments of known back arc setting. Although some geochemical data are available for these units, most analyses are from the Matsue Formation around Matsue, and the Omori, Jinzai, and Fujina Formations in the Lake Jinzai area to the west (Fig. 1; Roser *et al.,* 2001).

This paper reports whole-rock major and trace elements analyses of sandstones, mudrocks, and a few volcanic rocks from the Kawai-Kuri, Omori, and Fujina Formations collected from a strip along the coast of Lake Shinji between Shinji and Matsue, and of Ushikiri Formation sandstones and mudstones from Shimane Peninsula. These data supplement the analyses in Roser *et al.* (2001), and hence contribute to a growing database for back arc sediments in Shimane. The main purpose of this report is describe the sample suites and to present the data. Detailed discussion of its significance will be given in future publications, when data are available for all units in the succession.

Geology

Schematic stratigraphy of the Miocene succession in NE Shimane is given in Fig. 2. General description of each unit is given by Roser *et al.* (2001), and only a summary of the units analyzed here is given below.

Kawai and Kuri Formations

The Kawai and Kuri Formations crop out intermittently in lowland areas south of Lake Shinji. The main lithologies present in the Kawai Formation are arkosic arenites, conglomerates, andesitic to dacitic volcanics, subaqueous pyroclastic flow deposits, and volcaniclastic sediments. The

*Dept. of Geoscience, Shimane University, 1060 Nishikawatsu, Matsue 690-8504, Japan.

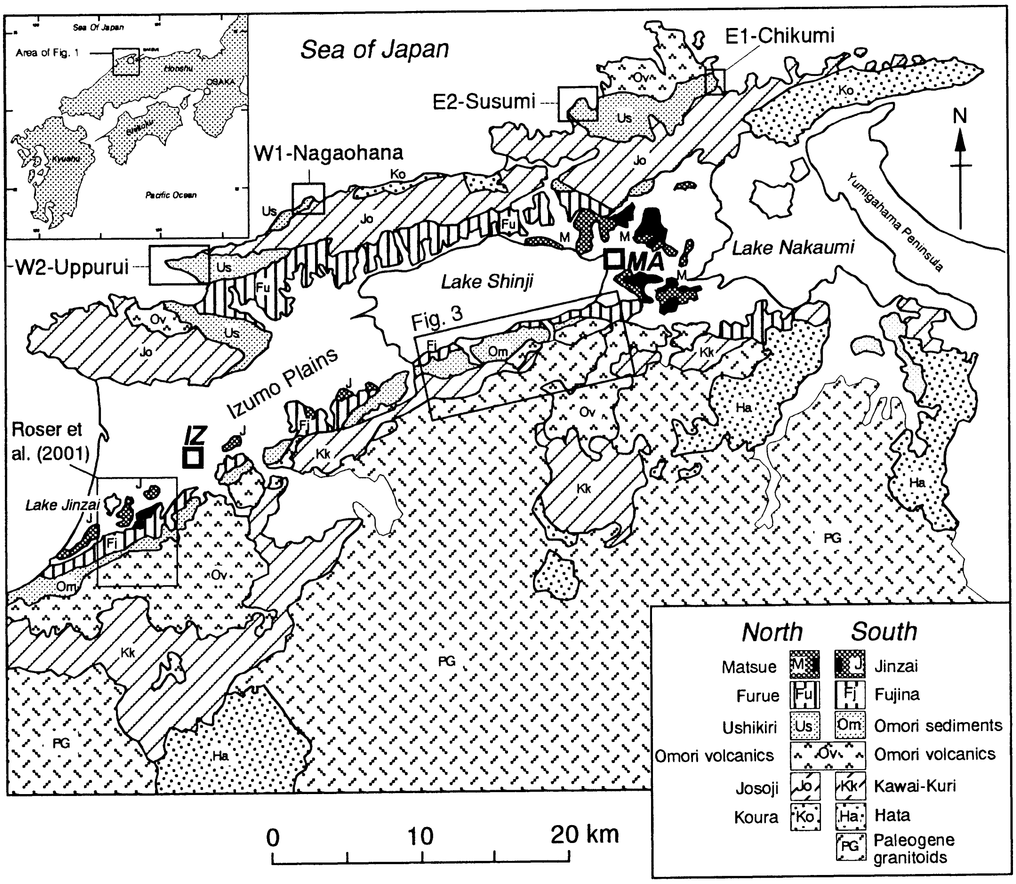

Fig. 1. Map showing the locations of the areas sampled and generalized distribution of Miocene sedimentary and volcanic rock units in the Matsue-Izumo district. Geology based on the 1 : 200 000 geological map of Shimane Prefecture (Editorial Board of Geological map of Shimane Prefecture [EBGMSP], 1997). Boxes W1, W2, E1, E2 - collection sites of Ushikiri Formation; box south of Lake Shinji shows the area of Fig. 3, from which samples of the Kawai-Kuri, Omori, and Fujina Formations were collected. Box to the west around Lake Jinzai is the area examined by Roser *et al.* (2001). Formation names in the legend are applied to the north (Shimane Peninsula) and south of Lake Shinji, respectively. Square *IZ* - Izumo city; *MA* - Matsue. Inset: location in Japan.

Kuri Formation mainly comprises mudstone and dacitic to rhyolitic lavas and subaqueous pyroclastic flow deposits.

The Kawai Formation was deposited in a beach to continental edge environment, and grades into Kuri Formation (Kano *et al.,* 1991). Based on the presence of benthic foraminifera, Kuri Formation was deposited in a continental shelf to bathyal environment (Kano *et al.,* 1994). Radiometric ages of Kawai volcanics generally lie in the range 15-19 Ma (Kano *et al.,* 1998). The two formations are almost contemporaneous, and they intertongue in places (Kano *et al.,* 1991, 1994). Consequently, for the purposes of this study, they are here grouped as the Kawai-Kuri Formation.

Omori Formation

Omori Formation rocks unconformably overlie the Kawai -Kuri Formation, and crop out in a discontinuous strip between Izumo and Matsue (Fig. 1). Deposition was terrestrial to shallow marine. The main lithologies are calcalkaline andesitic to dacitic terrestrial lavas and hayaloclastites, conglomerates, sandstones, and siltstones, in ascending stratigraphic order. In the Shinji-Matsue area sampled here (Fig. 1), well-jointed andesitic lavas tend to occur in the west, and hyaloclastites in the east. The lavas contain augite and hypersthene, and are plagioclase-rich. Reported ages from Omori volcanic rocks range from ~13 to 16 Ma (Morris *et al.,* 1990; Kano *et al.,* 1998).

Overlying conglomerates consist mainly of subangular to rounded granule- to cobble-sized andesite clasts. The conglomerates are succeeded by tuffaceous sandstones. Around Kimachi (Fig. 3) this horizon is referred to as Kimachi stone, which is used extensively as a building and decorative stone. Kimachi stone is a fine to medium grained, highly lithic sandstone. Lithic fragments are mainly volcanic (andesite, dacite, rhyolite, and tuff) and derived directly from the underlying Omori volcanic lithotypes, although granitic and porphyry fragments also occur. Plagioclase, clinopyroxene, ferromagnesian minerals and glass also occur as individual mineral fragments, set in a matrix of zeolite, chlorite, glass, and other material (Sawada, 2000). The Kimachi horizon passes upward into fine-grained sandstones that may contain shell fossils.

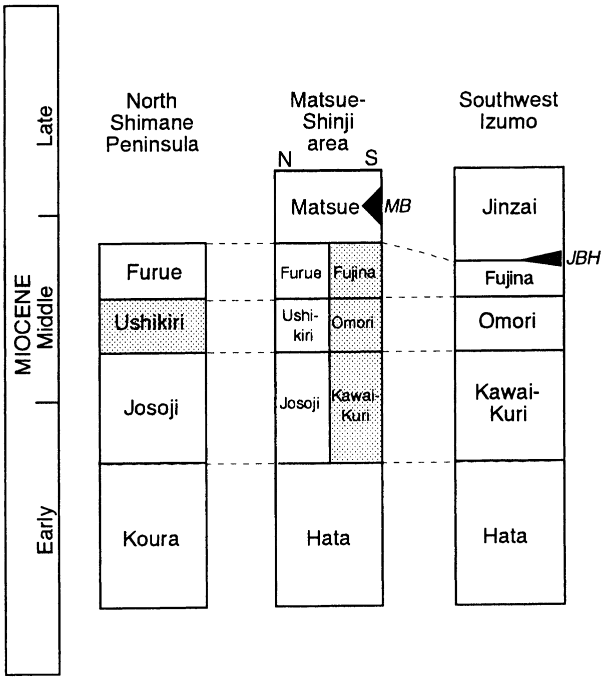

Fig. 2. Schematic stratigraphy and correlations between formations in Shimane Peninsula and the Matsue-Shinji and Izumo districts. Shaded formations are those sampled in this study. Abbreviations: *MB* - Matsue Basalt; *JBH* - Jinzai Basalt Horizon. Based on Kano *et al.* (1989, 1991, 1994, 1998), EBGMSP (1997) and Yamauchi (*pers. comm.* 2001).

Ushikiri Formation

Ushikiri Formation crops out extensively in Shimane Peninsula, where it consists of submarine volcanic rocks (andesite-rhyolite), tuffs, conglomerates, sandstones, and mudrocks. Tuff in the upper Ushikiri Formation has been dated at 14.3 ± 1.4 Ma (Kano *et al.,* 1989), and planktonic foraminifera indicate deposition during zone N 9 (Blow, 1969), equivalent to 14.8-15.1 Ma (Kano *et al.,* 1991). The Ushikiri rocks are thus a deeper-water correlative of the terrestrial to shallow water Omori Formation. Deposition is thought to have occurred in shallow water to bathyal zones. Benthic foraminifera suggest a continental shelf and slope environment.

Sedimentation began on the flanks of active submarine volcanic edifices, along with subaqueous pyroclastic activity, leading to deposition of mass flow and turbiditic volcaniclastic sediments (Takayasu *et al.,* 1992; Kano *et al.,* 1994). In Shimane Peninsula, thicknesses and abundances of conglomerates decrease from west to east, and thinner, fine-grained sediments become more dominant. Acid tuffs and tuffaceous sandstones are also prominent in the east (Kano *et al.,* 1994). Lithologic changes, flute casts, and direction of ripple currents suggest derivation of much of the western part from underlying andesitic volcanics (Kano *et al.,* 1991), and subsequent dispersion mainly to the east, as turbidity currents. However, current marks in the eastern part suggest transport to the south or west. Many of the turbidite sandstones contain mud clasts, entrained from underlying muds (Kano & Takeuchi, 1989).

Fujina Formation

Fujina Formation sediments conformably overlie those of the Omori Formation, but may also onlap Omori volcanic rocks. Fujina rocks crop out along the shore of Lake Shinji between Shinji and Matsue, and toward Izumo (Fig. 1). The main lithologies are fine to very fine-grained sandstones, siltstones, and mudstones. Sandstones and siltstones near the boundary with Omori Formation contain marine macrofossils (e.g. *Phacosoma, Glycymeris, Kotorapecten*) and carbonate nodules (Ogasawara and Nomura, 1980). Plant material and bioturbation is also common. Alternations of siltstone and fine sandstone sometimes show large-scale water-escape structures (Kano *et al.,* 1991). In the study area (Fig. 3), sandstones are more common west of Yumachi, whereas siltstones and mudstones dominate to the east. The depositional environment is interpreted as shallow marine to shelf, based on the occurrence of shell fossils and planktonic foraminifera. The age of Fujina Formation is estimated to be 12-14 Ma, based on correlation with planktonic foraminifera zones N 10-N 11 (Kano *et al.,* 1994).

Sample Suites

Kawai-Kuri, Omori, and Fujina Formations

Samples from the Kawai-Kuri, Omori, and Fujina Formations were collected from 46 sites in a 16 x 4 km strip between Shinji and Matsue (Fig. 1). Geology and sample localities are given in Fig. 3; more detailed description of individual sites is given in Fujii (2003). Samples were divided into groups according to their lithofacies and stratigraphic position within each formation, i.e. K1-4 (Kawai-Kuri), O1-5 (Omori), and F1-3 (Fujina), from base to top.

Samples from the lower part of the Kawai-Kuri sedimentary succession (K1) were collected from four locations (Table 1). All were coarse- to very coarse-grained laminated arkosic sandstones containing abundant angular quartz, plagioclase, and K-feldspar, and occasional subrounded clasts of granite and lesser dacite. Samples from the middle Kawai-Kuri (K2) were also arkosic, but were considerably finer grained than in K1. Outcrops at two sites consisted of alternating beds of plane-laminated very fine to medium grained sandstones, along with lesser siltstones and mudstones. The coarser sandstones contained some granitic granules. Flow-banded rhyolite (K3) was collected at one site (33), but not analysed. Uppermost Kawai-Kuri samples (K4) were collected at three sites a short distance below overlying Omori Formation conglomerates. All were well-bedded, somewhat bleached mudstones and siltstones, in contrast to the arkosic sands present lower in the formation.

Omori andesite lavas (O1) were collected at two sites.

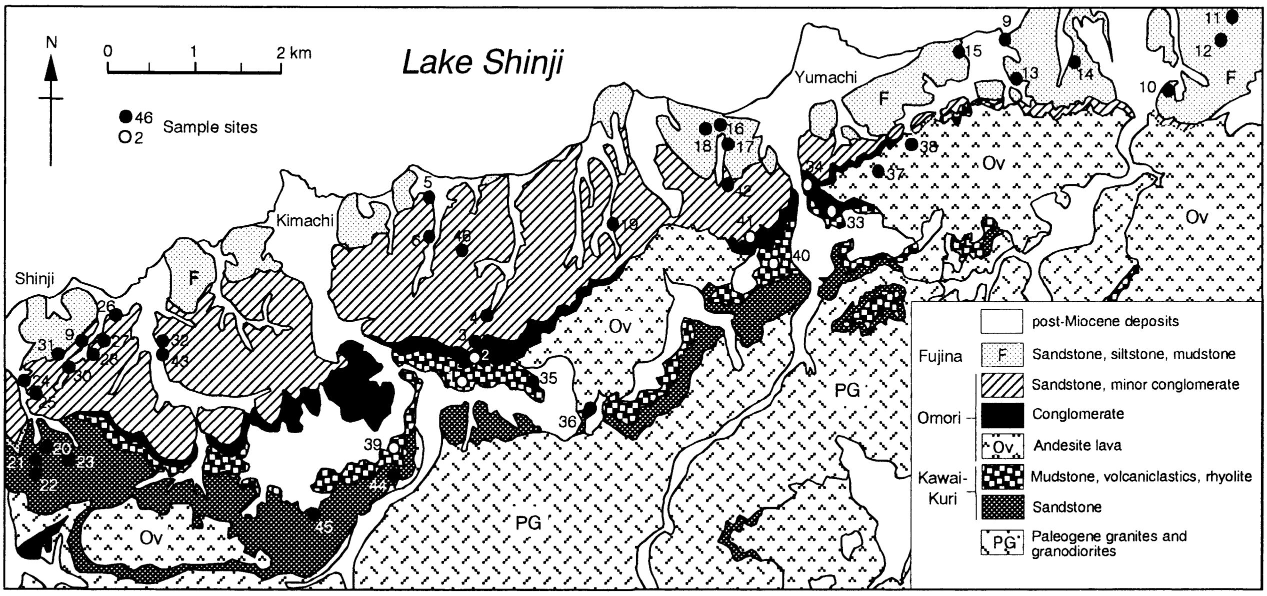

Fig. 3. Sample locations and geology of the area south of Lake Shinji. Geology based on Kano *et al.* (1991, 1994).

These samples contained abundant plagioclase phenocrysts and glomeroporphyritic hypersthene and hornblende, set in an olive green glassy groundmass. Although outcrop was limited, samples were collected from the conglomeratic facies (O2) at two sites. At site 2, the base of the outcrop consisted of grey, poorly laminated coarse sandstone. This was overlain by two thin (1.35 and 1.5 m) boulder to cobble conglomerates containing subrounded to subangular clasts of andesite, dacite, and minor sandstone/mudstone. The lower unit exhibited weak inverse grading. Several conglomerate outcrops examined higher in the sequence were clast-supported pebble to cobble conglomerates, again dominated by andesitic detritus. Six samples were collected from the lower Omori sandstone facies (O3). These were generally massive, white to brownish, medium to coarse grained sandstones; finer size grades were lacking.

Kimachi stone facies (O4) samples were taken from a quarry (Katsube Sekizaiten). The quarry face comprised weakly graded or massive medium to coarse grey sandstone. Intercalated mud was very rare, and was confined to a few isolated streaks a few mm thick and tens of centimeters long. The sandstones were poorly sorted, and contained plagioclase, hornblende, volcanic glass, K-feldspar, clinopyroxene, and opaque oxides as discrete grains, along with abundant volcanic rock fragments (andesite, rhyolite, and tuff). Secondary zeolites were also common. Andesitic rock fragments exhibited both microlitic and glassy groundmasses, and rhyolite fragments perlitic structure. The Kimachi facies grades up into O5 (Upper Omori sandstone facies), which are mainly fine or very fine grained sandstones, some of which are contain concretionary horizons. Broken shell fragments were also observed in non-cemented sandstones at these outcrops.

The Fujina Formation samples were divided into three groups based on stratigraphic position. Lower Fujina (F1) samples were collected from the sandstone-mudstone zone at sites 16-18 (Fig. 3). Samples ranged from medium sandstone through to mudstone. Bioturbation, shell fragments, and plant material were common. Middle Fujina (F2) samples represent the lower part of the Fujina siltstone/mudstone zone. All were massive blue-grey siltstone to very fine sandstone containing some plant fragments, along with Fe-oxide pans and blue Mn oxyhydroxide coatings. Samples from the uppermost part of the Fujina Formation (F3) were collected from isolated outcrops in the outskirts of Matsue City. Grain size ranged from very fine sand through to mud. As in the rest of this formation, bioturbation and plant fragments were common. Concretionary horizons also occurred at one locality.

Ushikiri Formation

Ushikiri sandstones and mudstones were collected from shore platform exposures at four sites on Shimane Peninsula (Fig. 1). Sketch columns and sample positions are given in Hashimoto (2003).

(a) East Shimane Peninsula

Fifteen samples (HS 1-15, numbered from base to top) were collected from a 40 m thick turbidite succession at Chikumi (E1). This represents the middle to lower part of the Ushikiri Formation. Sandstone beds ranged from 1-120 cm in thickness. Most were fine to medium grained, although a few very coarse grained beds were also present. Interbedded mudstones ranged from 20 cm to 100 cm in thickness. Some beds displayed T_b-T_c Bouma sequences, and both parallel and cross lamination were observed. Overall sandstone to mudstone ratio was 30:70. In thin section, the sandstones contained abundant sericitized plagioclase and angular to subrounded volcanic rock fragments 0.1-0.2 mm in diameter. The latter were mainly andesitic. Subordinate detrital quartz was also present. Many rock fragments and feldspar grains were partially converted to calcite and zeolite, which also formed cements and replaced matrix.

Samples were collected from three exposures in the Susumi area (E2), one at Mitsu (Kashima-cho), and two at Susumi (Shimane-cho). These represent the lower part of Ushikiri Formation. Three samples (HS 16-18; two sandstones, one mudstone) were collected at Mitsu. Sandstone beds ranged from 5-210 cm in thickness, and were mainly fine and medium grained. The mudstones (10-80 cm thick) at this site were purplish, possibly due to thermal metamorphism from nearby intrusive and volcanic rocks. Sandstone to mudstone ratio at Mitsu was ~50:50. Twelve samples (HS 19-30) were collected from 30 and 25 m thick sections of alternating sandstones and siltstones at Susumi. The sandstones here were generally fine to medium grained, normally graded tudbidites 1-120 cm in thickness. Some beds displayed slump structures. Interbedded siltstones ranged from 10 to 70 cm in thickness, and overall sandstone:siltstone ratio was 40:60.

(b) West Shimane Peninsula

Beds at both localities sampled in west Shimane Peninsula are generally thicker than those in the east, and sandstones are coarser. Fifteen samples were collected from a single 80 m-thick succession of alternating sandstones and mudstones at Nagaohana (W1), in the upper part of the Ushikiri Formation. The sandstones are mostly pale grey, medium grained beds 2-170 cm thick. Slump structures and groove casts are common in this section. Rip-up clasts of mudstone, siltstone and very fine sandstones also occur frequently. Interbedded mudrocks were mostly siltstone, ranging from 7 cm to 40 cm in thickness. Sandstone: siltstone ratio was about 70:30. In thin section the sandstones consist mainly of plagioclase and andesitic-dacitic volcanic rock fragments, often chloritized and epidotized, and lesser quartz. Calcite is common, both as cement and as an alteration product.

The remaining 13 samples (HS 46-58) were collected from three outcrops around Uppurui (W2). HS 47-54 were from the lower part of Ushikiri Formation, whereas HS 46 and HS 55-58 represent the middle part. The sedimentary succession at which samples HS 47-54 were collected consisted of 2-30 cm beds of fine to coarse sandstones interbedded with thin (1-10 cm) mudstones. These were overlain by a 2 m thick conglomerate bed consisting of subrounded dacite, andesite, and sandstone clasts ranging from 5 to 50 cm in diameter. Weak imbrication suggests transport direction from SE to NW.

Analytical Methods

Indurated samples were manually chipped to <1 cm with a splitter to remove surficial rinds and veins if present. The chip was then repeatedly soaked in deionized water to remove dust and/or sea salt, and subsequently dried in an oven at 110℃. Unconsolidated samples, primarily fine sandstones and mudrocks from the Fujina and upper Omori Formation, were handled in the same way, but carefully decanted to avoid loss of fines. Some of these samples had suffered mild pervasive weathering, and complete removal of all weathered material was impractical.

The dried samples were subsequently crushed in a tungsten carbide ring mill for 30-45 seconds (Roser *et al.,* 1998). Sample weights were generally 75-150 g. Ten gram subsamples were dried at 110℃ for at least 24 hours before gravimetric determination of loss on ignition (LOI; 2+ hours at 1000℃). The ignited material from the LOI determinations was then hand-ground in an agate pestle and mortar and returned to a 110℃ oven before preparation of fusion beads for X-ray fluorescence (XRF) analysis.

XRF analyses were made using the Rigaku RIX-2000 instrument at Shimane University. Both major and trace element determinations were made on glass fusion beads prepared with an alkali flux consisting of 80% lithium tetraborate and 20% lithium metaborate, and flux to sample ratio of 2:1, following the method of Kimura and Yamada (1996). Additional details of the analytical methods used are given in Roser *et al.* (2000, 2001).

Results and Discussion

Analyses are listed in Table 1 (Kawai-Kuri, Omori, and Fujina Formations) and Table 2 (Ushikiri Formation), on a hydrous basis. Some contrasts in geochemical composition are evident between formations and lithotypes.

Kawai-Kuri sandstones tend to be silica-rich, with SiO_2 abundances ranging from 66.5-83.5 wt%, with highest abundances in the coarser varieties (Table 1). K_2O abundances are relatively high (3.5-5.0 wt%), with K_2O > Na_2O, and CaO low (with one exception, <1 wt%). MnO and P_2O_5 contents are also conspicuously low (generally < 0.03 wt%). Ba is the most abundant trace element (>400 ppm), although high abundances of Zr (>300 ppm) also occur in a few samples. As is typical of silicic sediments, SiO_2 contents of Kawai-Kuri mudrocks are generally less than in the sandstones, but show considerable range (59.2-76.7 wt%) and overlap with the compositions of the finer sandstones.

In contrast to Kawai-Kuri sandstones, Omori equivalents have relatively uniform compositions. With the exception of three concretionary samples enriched in CaO, SiO_2 contents range from 52.8 to 68.1 wt%, but most lie in the narrower range of 58-64 wt%. Among the other elements, Na_2O is generally greater than K_2O, and Fe_2O_3 contents are more

Table 1. Whole–rock XRF analyses of sedimentary and volcanic rocks from the Kawai–Kuri, Omori, and Fujina Formations, Shinji–Matsue. Major elements wt%, trace elements ppm.

SaNr	Group	Site	Lithology	SiO_2	TiO_2	Al_2O_3	Fe_2O_3	MnO	MgO	CaO	Na_2O	K_2O	P_2O_5	LOI	Total	Ba	Ce	Cr	Ga	Nb	Ni	Pb	Rb	Sc	Sr	Th	V	Y	Zr
Fujina Formation																													
FR-6	F3(U)	9	vf sst	71.35	0.66	14.22	4.07	0.02	1.30	0.55	1.26	2.61	0.08	3.94	100.05	403	69	54	15	8	26	23	108	12.9	121	8.9	101	32	266
FR-7	F3(U)	9	vf sst	71.75	0.65	14.44	3.52	0.02	1.14	0.48	1.19	2.56	0.09	4.18	100.01	444	100	52	14	9	41	22	104	11.4	118	8.7	96	58	274
FR-8	F3(U)	9	conc sst	51.87	0.48	9.19	3.29	0.33	1.05	15.63	0.88	1.95	0.07	13.48	98.21	306	48	31	9	9	37	12	67	8.8	130	7.2	57	89	196
FR-12	F3(U)	11	mst	72.87	0.58	13.36	2.02	0.02	0.77	0.73	1.67	2.80	0.05	4.69	99.55	430	137	35	13	8	8	16	91	9.3	140	7.9	73	44	328
FR-13	F3(U)	11	vf sst	70.99	0.67	16.60	3.09	0.01	1.17	0.46	1.12	2.91	0.11	2.68	99.81	399	247	50	18	11	17	18	109	14.4	106	10.0	121	86	195
FR-14	F3(U)	11	vf sst	76.41	0.58	13.04	3.30	0.02	0.85	0.75	1.62	2.85	0.07	0.40	99.89	470	66	34	13	7	13	17	96	8.5	151	6.1	77	29	288
FR-15	F3(U)	12	vf-f sst	72.01	0.70	15.58	3.03	0.00	1.02	0.19	0.75	2.46	0.04	4.19	99.98	387	77	55	16	9	11	19	99	14.2	88	9.3	102	32	243
FR-18	F3(U)	15	zst-vf sst	70.26	0.73	17.44	2.91	0.00	1.06	0.09	0.24	2.16	0.02	5.39	100.30	338	63	54	16	8	11	16	90	17.0	51	7.9	113	23	248
FR-19	F3(U)	15	zst-vf sst	73.84	0.71	14.72	2.59	0.00	0.97	0.14	0.62	2.31	0.03	4.07	99.99	391	71	52	15	8	12	15	90	15.0	73	9.6	98	20	280
FR-10	F2(M)	10	zst-vf sst	70.35	0.58	13.94	4.41	0.02	1.41	1.00	1.30	2.63	0.06	4.13	99.83	438	64	38	15	7	34	20	100	12.7	150	7.2	92	25	198
FR-11	F2(M)	10	zst-vf sst	70.60	0.60	14.13	4.27	0.02	1.38	0.89	1.31	2.66	0.06	4.02	99.93	405	69	41	15	7	30	20	102	13.8	143	8.1	97	30	229
FR-16	F2(M)	13	zst-vf sst	71.39	0.57	16.46	2.82	0.01	0.89	0.19	0.55	2.48	0.02	4.64	100.02	392	57	33	15	6	8	15	92	12.4	64	6.7	83	14	229
FR-17	F2(M)	14	vf sst	72.88	0.58	14.97	2.35	0.01	1.06	0.60	1.42	2.75	0.04	3.33	99.99	436	54	44	15	6	11	15	95	10.8	129	7.7	80	20	223
FR-20	F1(L)	16	m sst	72.32	0.56	16.51	2.40	0.01	0.64	0.19	0.39	1.87	0.01	5.14	100.03	320	45	25	15	6	10	13	70	12.5	51	5.5	77	25	204
FR-21	F1(L)	16	zst-vf sst	69.83	0.68	17.68	3.04	0.00	1.10	0.09	0.04	2.11	0.02	5.57	100.16	295	58	55	17	8	8	17	87	14.0	40	7.3	103	27	252
FR-22	F1(L)	17	mst	72.04	0.65	14.68	2.41	0.01	1.01	0.53	1.39	2.64	0.08	4.16	99.59	853	105	49	16	9	14	21	99	11.0	174	7.6	96	53	239
FR-23	F1(L)	18	vf sst	69.02	0.71	18.06	2.83	0.01	1.16	0.08	0.03	2.20	0.02	5.68	99.79	299	46	46	18	8	8	15	92	15.4	42	8.0	106	18	227
Omori Formation																													
FR-33	O5(U)	26	f sst	68.09	0.75	18.67	2.89	0.01	1.10	0.10	0.27	1.90	0.02	6.39	100.18	250	54	52	19	8	3	13	80	20.0	36	7.9	124	19	205
FR-34	O5(U)	29	c-vc sst	65.39	0.62	15.24	4.85	0.05	1.28	4.17	2.37	1.96	0.17	3.99	100.10	343	39	1	14	5	3	15	52	18.2	617	4.0	112	25	121
FR-35	O5(U)	31	conc sst	32.52	0.57	9.12	5.21	0.53	1.92	27.39	1.14	0.77	0.23	19.59	99.00	153	35	13	9	4	6	9	21	10.0	303	2.9	73	17	76
FR-36	O5(U)	31	vf sst	66.50	0.61	14.38	5.10	0.03	1.77	2.74	2.10	2.16	0.09	4.37	99.86	416	50	25	15	6	14	17	80	12.7	285	6.8	100	21	176
FR-44	O5(U)	31	conc sst	32.17	0.40	7.82	4.72	0.63	1.96	28.31	0.90	0.85	0.25	20.70	98.71	149	40	13	7	4	8	9	24	6.9	252	4.8	72	19	84
FR-44b	O5(U)	31	conc sst	29.48	0.42	6.65	4.27	0.58	1.43	30.99	0.77	1.08	0.58	22.88	99.14	147	26	18	7	3	5	7	31	4.0	245	4.3	57	12	96
FR-55	O4(K)	46	f-c sst	52.76	2.02	12.97	17.07	0.22	3.34	4.84	2.69	1.16	0.18	2.72	99.95	254	27	41	18	5	9	12	28	28.2	266	3.7	652	21	113
FR-56	O4(K)	46	f-c sst	62.73	0.67	15.24	5.92	0.12	2.14	5.08	3.18	1.47	0.16	3.41	100.13	312	33	5	15	4	5	15	41	21.8	332	4.3	116	24	118
FR-57	O4(K)	46	f-c sst	61.06	0.69	15.46	6.57	0.13	2.37	5.48	3.23	1.41	0.16	3.41	99.96	298	33	5	15	5	4	15	37	23.2	342	2.8	133	23	118
FR-58	O4(K)	46	mst	67.99	0.48	11.88	6.95	0.20	2.66	2.87	1.51	1.32	0.08	4.17	100.12	204	34	15	13	5	17	11	58	14.9	166	4.8	113	18	111
FR-59	O4(K)	KM	f-c sst	60.55	0.69	15.59	6.85	0.13	2.52	5.44	3.22	1.50	0.15	3.11	99.75	302	31	16	15	4	3	12	36	21.9	316	3.0	138	23	111
FR-60	O4(K)	KM	f-c sst	58.73	0.64	15.63	6.26	0.13	2.20	6.98	3.08	1.45	0.14	4.60	99.84	307	34	5	15	4	4	13	37	18.6	335	3.9	123	21	111
FR-24	O3(S)	19	m-c sst	62.91	0.63	15.05	6.71	0.07	1.62	4.45	2.29	1.48	0.14	4.77	100.13	323	36	5	14	4	3	13	41	22.4	312	3.0	127	30	112
FR-32	O3(S)	25	vc sst	55.80	0.91	15.96	7.34	0.21	2.54	8.31	2.61	1.07	0.32	4.79	99.85	306	32	6	16	4	3	10	35	23.2	466	4.9	146	20	94
FR-43	O3(S)	42	m sst	61.28	1.09	22.24	5.15	0.03	0.58	0.36	0.47	1.67	0.04	7.76	100.66	455	31	22	23	5	6	12	50	31.4	51	4.0	227	20	153
FR-45	O3(S)	32	c-m sst	63.14	0.73	15.78	6.75	0.08	1.00	4.28	2.56	1.83	0.13	4.00	100.26	386	33	11	16	5	9	15	51	20.5	467	3.6	144	35	117
FR-46	O3(S)	32	m sst	63.68	0.73	16.58	7.42	0.03	0.76	2.03	1.79	2.11	0.10	5.18	100.41	366	27	13	17	4	4	13	65	19.7	307	3.9	156	12	132
FR-47	O3(S)	43	m-c sst	60.46	0.72	14.29	6.80	0.08	2.47	4.90	2.10	1.88	0.17	6.04	99.88	333	28	10	14	5	3	13	45	24.8	536	2.4	141	25	113
FR-5	O2(C)	2	c-vc sst	64.87	1.22	19.10	4.82	0.03	0.77	0.89	1.13	2.11	0.03	5.38	100.35	434	31	5	22	6	6	17	51	33.3	121	5.0	219	19	174
FR-42	O2(C)	41	c sst	57.01	1.28	25.41	4.12	0.02	0.57	0.20	0.01	2.55	0.04	9.26	100.45	902	17	23	27	5	10	14	51	47.6	28	3.7	276	12	173
FR-40	O1(V)	37	andesite	61.67	0.78	16.43	6.06	0.11	2.03	6.48	2.90	2.42	0.24	0.54	99.67	468	46	17	17	5	5	11	67	22.5	368	5.3	184	30	128
FR-41	O1(V)	38	andesite	57.48	0.80	16.63	8.47	0.14	2.93	7.46	2.73	1.95	0.25	0.87	99.70	414	38	20	17	5	5	12	27	23.5	405	4.6	198	21	130
Kawai-Kuri Formation																													
FR-1	K4(U)	1	mst	76.69	0.47	11.29	1.78	0.01	1.01	0.08	0.23	2.87	0.03	5.00	99.46	270	40	50	14	5	16	57	96	14.0	32	8.4	124	11	95
FR-2	K4(U)	1	zst	76.34	0.51	11.93	1.73	0.00	1.12	0.10	0.20	3.30	0.02	4.37	99.64	296	49	57	15	7	11	26	104	13.2	37	11.1	113	17	114
FR-3	K4(U)	1	mst	78.12	0.44	11.30	1.64	0.00	1.21	0.12	0.23	2.19	0.03	4.65	99.93	302	43	52	14	6	13	41	85	13.0	42	7.9	100	14	102
FR-4	K4(U)	1	zst	68.49	0.34	17.92	2.43	0.01	2.72	0.28	0.13	0.53	0.02	6.55	99.42	211	73	5	18	6	10	16	18	9.5	70	10.0	31	33	199
FR-38	K4(U)	35	mst	72.14	0.63	15.15	3.20	0.00	1.53	0.08	0.19	2.58	0.03	4.68	100.22	334	57	53	20	8	8	38	120	15.0	37	10.6	118	26	127
FR-39	K4(U)	36	mst	66.62	0.85	18.71	3.70	0.01	1.77	0.17	0.10	2.42	0.03	5.99	100.36	311	55	55	22	9	10	25	115	26.2	45	10.5	162	24	145
FR-48	K2(M)	44	c-vc sst	78.10	0.21	11.99	1.34	0.02	0.34	0.57	1.48	3.37	0.01	1.95	99.39	402	64	8	12	5	2	23	91	4.1	100	8.5	28	7	85
FR-49	K2(M)	44	vf-f sst	66.48	1.07	17.27	2.45	0.02	1.51	0.72	1.52	4.38	0.03	4.25	99.70	460	49	1	25	8	7	15	109	23.4	112	4.9	109	44	168
FR-49b	K2(M)	44	mst	59.20	1.38	21.27	4.58	0.01	2.74	0.61	0.19	2.52	0.09	7.52	100.11	349	57	5	32	8	17	16	62	36.8	88	2.4	132	89	160
FR-50	K2(M)	44	m-c sst	80.85	0.15	10.78	0.56	0.02	0.37	0.41	1.30	3.82	0.01	1.08	99.35	463	22	1	11	4	1	19	107	0.1	86	6.0	6	9	75
FR-51	K2(M)	44	m sst	73.29	0.52	14.64	1.45	0.02	0.71	0.51	1.38	4.35	0.01	2.47	99.36	479	38	7	22	6	5	16	129	7.3	95	9.2	34	19	243
FR-51B	K2(M)	44	mst	64.16	1.01	19.25	2.67	0.03	1.32	0.53	0.81	3.95	0.01	5.16	98.91	403	65	15	42	11	12	24	136	20.1	89	19.6	89	47	333
FR-52	K2(M)	44	vf-f sst	69.49	0.61	16.24	2.36	0.03	0.85	0.42	1.21	4.95	0.01	3.22	99.39	510	53	12	20	7	7	19	147	8.0	79	10.3	42	19	389
FR-52b	K2(M)	44	mst	62.94	0.98	20.10	2.90	0.03	1.62	0.43	0.74	4.13	0.01	5.39	99.29	441	80	9	27	10	12	22	146	22.7	78	15.2	82	57	348
FR-53	K2(M)	44	f-m sst	66.72	0.62	17.92	3.05	0.04	1.23	0.38	0.99	4.49	0.01	4.19	99.64	501	42	8	22	7	7	22	143	10.7	70	7.0	53	27	204
FR-54	K2(M)	45	m sst	78.94	0.16	11.32	0.98	0.01	0.31	0.62	2.06	4.28	0.02	0.64	99.34	475	32	1	10	5	0	15	112	1.0	124	4.2	7	5	91
FR-25	K1(L)	20	vc sst	82.54	0.09	9.81	0.50	0.00	0.23	0.16	0.53	4.97	0.01	1.02	99.87	506	18	12	9	3	1	12	137	1.5	44	2.7	8	3	51
FR-26	K1(L)	21	vc sst	81.49	0.15	10.48	0.25	0.03	0.23	0.26	0.92	5.07	0.01	0.88	99.78	530	37	16	8	4	20	12	140	1.9	58	4.2	6	8	58
FR-27	K1(L)	22	vc sst	83.49	0.06	9.64	0.14	0.00	0.24	0.41	1.76	4.21	0.01	0.26	100.21	480	17	1	8	2	0	15	111	0.9	85	3.2	1	3	51
FR-31	K1(L)	23	c-vc sst	74.48	0.32	12.15	3.02	0.07	0.99	1.30	2.19	3.57	0.06	1.76	99.92	418	22	1	12	4	1	15	94	4.4	154	3.1	26	17	87

Notes: Column headings: SaNr=sample number. Group=lithofacies as described in the text, U=upper, M=middle, L=lower, K=Kimachi horizon, S=sandstone,V=volcanic. Site=site number (Fig. 3). LOI=loss on ignition. Total iron as Fe_2O_3.
Lithology abbreviations: sst=sandstone, zst=siltstone, mst=mudstone; vc, c, m f, vf=very coarse, coarse, medium, fine, and very fine, respectively; conc=concretionary.

than double those in Kawai Kuri equivalents (Table 2). Rb is also lower and Sr higher. Fujina sandstones and mudrocks have very uniform compositions. With one calcareous sample apart, SiO_2 contents range only from 70.3 to 76.4 wt%. As in the Kawai Kuri Formation, K_2O is > Na_2O, and CaO, MnO, and P_2O_5 contents are low. Fe_2O_3 and Sr contents are lower than in Omori sandstones, and Rb, Ce, Th, Y, and Zr higher.

The chemical contrasts between the formations and lithotypes can be conveniently illustrated using normalized multi-element diagrams (spidergrams) of average compositions. The normalizer used was the average Upper Continental Crust (UCC) composition of Taylor and McLennan (1985). Data were first normalized to 100% after deduction of LOI, and then normalized against UCC. Major elements were normalized as oxide wt%, and trace elements as ppm. Formation averages were then calculated for both sandstones and mudrocks (siltstones and mudstones). Samples with excessive CaO contents (>10 wt%) due to presence of authigenic or biogenic carbonate were omitted from the averages to avoid dilution effects. In the spidergrams elements are arranged from left to right in order of increased UCC-normalized abundances in the average Cenozoic greywacke of Condie (1993), following the method of Dinelli *et al.* (1999). This places many incompatible elements at left (e.g. Nb, K, Zr, Sr), and compatible ferromagnesian elements (Sc, Fe, Ti, Ni, Cr, V) to the right.

Average Kawai-Kuri sandstone is depleted relative to UCC for all elements except K_2O, Rb, and SiO_2; depletion if greatest for CaO, Sr, MgO, Cr and Ni (Fig. 4A). The pattern compares reasonably well with San'in granitoids, with all elements except Th and Na_2O plotting within their range. The Kawai-Kuri mudstone pattern is similar for some elements, particularly in the segments Nb-Zr and SiO_2-Ba (Fig. 4A). However, the mudrock average is more depleted than the sandstones for Na_2O and Sr, and is enriched to near UCC values for MgO and Ce. The largest contrast is seen in the segment Sc-V, all of which are enriched relative to the sands and are near UCC levels. This is most likely to be a sorting effect.

Patterns for average Omori sandstone and the single

Table 2. Whole–rock XRF analyses of sandstones, siltstones, mudstones, and a tuff from the Ushikiri Formation, Shimane Peninsula. Notes as in Table 1.

SaNr	Lith	SiO_2	TiO_2	Al_2O_3	Fe_2O_3	MnO	MgO	CaO	Na_2O	K_2O	P_2O_5	LOI	Total	Ba	Ce	Cr	Ga	Nb	Ni	Pb	Rb	Sc	Sr	Th	V	Y	Zr
E1 Chikumi																											
HS-1	mst	60.93	0.71	17.33	6.46	0.04	2.52	1.49	1.47	3.64	0.13	5.32	100.03	296	65	72	22	9	31	18	150	17.3	93	11.2	157	24	130
HS-2	zst	69.01	0.56	13.92	5.87	0.02	2.39	0.33	1.19	2.56	0.08	4.12	100.05	261	46	82	19	7	25	19	114	14.9	63	9.0	128	15	106
HS-3	m sst	43.96	0.48	17.62	6.11	0.26	2.30	13.92	3.72	1.02	0.16	9.06	98.63	217	28	1	14	3	1	14	20	9.9	417	2.9	46	11	68
HS-4	mst	69.98	0.53	13.66	4.16	0.03	1.84	1.53	2.05	2.23	0.08	3.84	99.93	212	75	6	18	6	11	17	19	13.7	72	10.3	32	34	205
HS-5	m sst	58.63	0.88	17.04	7.13	0.08	3.42	2.86	5.28	0.75	0.21	4.23	100.52	253	34	10	16	4	4	13	20	21.9	304	2.5	125	21	100
HS-6	m sst	71.09	0.41	12.88	3.91	0.04	2.43	2.16	1.95	1.28	0.13	3.48	99.74	311	48	6	11	5	3	21	39	11.1	161	6.8	39	22	144
HS-7	zst	67.19	0.60	15.07	5.16	0.04	2.77	0.57	1.41	2.95	0.08	4.19	100.05	416	55	67	18	7	27	16	134	16.0	100	10.0	143	19	111
HS-8	f sst	55.63	0.69	17.77	7.99	0.10	5.64	3.37	3.90	0.46	0.24	4.20	99.98	475	25	59	17	5	21	10	12	22.8	342	4.5	175	17	89
HS-9	zst	73.10	0.50	11.76	4.23	0.03	1.85	1.45	1.73	1.84	0.11	3.22	99.82	450	38	37	14	5	14	10	77	14.5	151	5.9	117	15	91
HS-10	c -f sst	43.46	0.69	14.51	4.80	0.47	1.32	17.18	4.15	0.51	0.24	11.00	98.34	426	25	5	12	4	2	9	7	12.9	435	3.1	66	20	71
HS-11	zst	67.23	0.60	14.68	5.15	0.03	2.15	1.13	1.27	3.36	0.09	4.29	99.98	544	51	71	17	7	29	18	135	14.4	100	10.3	152	21	115
HS-12	zst	69.08	0.53	13.20	5.19	0.03	2.00	1.43	1.30	2.57	0.10	4.30	99.74	473	50	59	16	6	25	13	104	14.0	109	7.1	112	19	109
HS-13	m sst	71.09	0.56	12.21	4.68	0.04	1.11	1.97	2.58	1.63	0.09	4.07	100.03	562	32	32	12	5	14	6	58	17.6	209	3.6	103	16	101
HS-14	cse tuff	77.84	0.23	8.19	0.84	0.11	0.70	4.29	1.27	1.02	0.05	4.51	99.04	299	30	4	4	5	1	7	32	5.6	138	4.4	21	11	93
HS-15	mst	73.38	0.48	11.72	4.55	0.03	1.75	0.70	1.05	2.14	0.08	4.17	100.04	348	43	62	15	6	25	12	99	11.1	88	7.0	112	17	96
E2 Susumi																											
HS-16	m sst	72.01	0.49	14.44	3.53	0.03	1.14	0.89	4.66	1.74	0.13	1.29	100.35	557	34	6	8	4	5	15	61	13.4	219	4.1	32	16	92
HS-17	c-f sst	68.57	0.55	15.70	5.00	0.04	1.48	0.96	4.68	1.72	0.14	1.79	100.61	423	38	8	12	5	14	34	62	16.6	201	5.0	68	20	115
HS-18	zst	64.56	0.75	17.14	7.36	0.02	2.21	0.50	0.84	3.62	0.10	3.30	100.40	380	68	71	23	9	28	31	154	18.4	35	13.8	150	23	141
HS-19	m sst	55.17	0.89	15.81	8.66	0.07	2.94	7.18	2.31	1.31	0.28	5.33	99.95	368	33	14	17	5	7	13	30	23.6	296	3.9	186	20	105
HS-20	mst	64.07	0.68	14.72	7.47	0.04	2.50	1.67	1.23	2.93	0.50	4.47	100.27	377	48	46	18	7	23	20	117	17.7	120	7.8	156	24	115
HS-21	m sst	54.69	0.68	14.66	6.90	0.24	2.06	8.63	3.05	1.37	0.14	7.44	99.85	370	38	11	14	4	6	13	34	18.8	232	3.3	122	22	110
HS22	zst	64.54	0.66	15.90	6.63	0.03	2.13	1.54	1.81	2.85	0.13	4.05	100.27	385	48	34	18	6	17	18	93	19.8	131	6.7	140	23	128
HS23	f sst	57.21	0.94	15.29	7.16	0.18	2.66	5.87	3.91	0.99	0.15	5.62	99.99	309	35	14	14	5	6	12	22	26.8	251	3.9	177	22	123
HS24	f sst	65.53	0.64	15.57	6.12	0.03	2.11	1.50	1.94	2.70	0.11	3.96	100.21	429	42	29	18	5	14	17	85	17.9	143	7.1	148	21	124
HS25	mst	69.40	0.56	12.87	5.97	0.04	2.15	0.50	1.09	2.39	0.08	5.05	100.09	304	42	79	18	6	27	9	100	15.5	70	8.1	139	19	109
HS26	m sst	60.63	0.73	15.19	6.99	0.08	2.74	4.04	3.80	1.17	0.15	4.72	100.24	339	34	16	14	4	5	13	28	22.2	290	4.1	144	20	116
HS27	zst	69.03	0.49	11.91	5.83	0.06	1.86	2.03	1.03	2.08	0.17	5.53	100.01	274	51	60	17	6	20	10	87	14.2	88	7.0	115	24	101
HS28	zst	72.76	0.51	11.67	5.46	0.03	1.73	0.59	1.43	1.82	0.06	4.15	100.21	284	23	44	15	5	18	14	73	15.2	85	6.6	191	12	95
HS-29	f sst	64.50	0.51	12.32	2.81	0.08	1.10	6.68	3.45	1.82	0.12	6.03	99.41	415	36	9	8	4	4	12	41	13.9	286	2.8	52	23	99
HS-30	f sst	61.62	0.57	11.80	2.83	0.19	1.06	8.83	3.29	1.56	0.12	7.48	99.35	386	34	10	8	4	5	11	36	16.4	286	3.7	52	20	95
W1 Nagaohana																											
HS-31	f sst	52.13	0.73	15.21	6.74	0.22	2.36	9.08	3.99	1.10	0.14	8.32	100.03	243	29	14	12	4	5	12	15	23.9	332	2.8	154	22	99
HS-32	mst	66.40	0.63	14.97	6.26	0.05	2.06	0.98	1.85	3.10	0.10	3.96	100.36	460	46	35	19	6	17	14	102	18.6	142	7.0	139	24	121
HS-33	mst	65.33	0.63	15.31	6.43	0.05	2.13	1.15	1.70	3.21	0.10	4.26	100.30	531	49	34	19	6	16	11	102	17.7	149	8.0	143	24	127
HS-34	vf sst	71.44	0.49	12.69	5.96	0.04	1.87	0.85	1.99	1.68	0.08	3.44	100.53	235	33	30	15	4	13	9	62	14.5	137	4.7	120	13	97
HS-35	f sst	48.27	0.58	13.05	9.70	0.20	2.76	11.25	2.61	0.95	0.34	10.19	99.91	189	55	10	13	5	5	17	22	14.4	312	5.5	78	32	114
HS-36	zst	67.67	0.66	15.06	4.85	0.03	1.57	1.33	2.13	2.59	0.09	4.22	100.20	376	32	32	17	5	14	9	85	19.4	175	6.5	144	17	120
HS-37	m sst	47.69	0.70	16.41	7.21	0.23	2.36	11.35	3.55	1.39	0.15	8.91	99.95	338	42	8	15	5	6	15	27	23.3	344	3.9	132	24	111
HS-38	f sst	69.55	0.55	13.51	5.72	0.03	1.88	1.28	1.82	2.10	0.34	3.52	100.30	288	43	30	17	6	12	11	74	20.0	133	5.2	176	27	108
HS-39	zst	65.74	0.66	15.59	6.03	0.04	2.02	1.26	1.91	2.82	0.12	4.08	100.26	447	48	41	19	6	16	19	95	18.1	154	8.2	132	22	129
HS-40	m sst	58.77	0.79	18.26	8.16	0.06	2.73	2.72	4.53	1.28	0.16	3.30	100.75	277	36	19	16	5	6	15	26	24.9	327	2.9	173	23	127
HS-41	mst	59.92	0.71	16.87	9.26	0.05	3.35	0.97	1.14	3.29	0.28	4.88	100.72	299	53	58	25	9	21	11	125	21.4	71	10.9	192	31	137
HS-42	c-m sst	44.13	0.85	14.19	6.84	0.22	2.12	15.10	3.31	1.14	0.18	11.48	99.54	265	36	12	13	4	6	13	19	24.3	269	4.1	156	25	111
HS-43	vf sst	69.97	0.56	13.70	5.68	0.04	1.77	0.91	1.55	2.36	0.13	3.72	100.39	310	36	41	18	6	17	38	86	16.6	114	6.1	125	20	109
HS-44	m sst	48.29	0.87	15.15	7.45	0.26	2.40	11.59	3.46	1.12	0.14	9.03	99.76	270	31	20	15	4	6	10	20	23.4	299	3.3	171	21	115
HS-45	zst	71.13	0.56	12.90	5.58	0.04	1.77	0.84	1.68	2.03	0.08	3.65	100.26	273	41	37	16	6	16	12	77	16.0	121	6.7	127	17	108
W2 Uppurui																											
HS-46	vf sst	69.15	0.59	12.90	4.22	0.04	1.68	1.75	1.81	3.08	0.12	4.48	99.82	409	35	17	15	5	11	10	95	13.5	484	5.8	100	18	113
HS-47	f sst	67.93	0.56	14.36	4.31	0.05	1.58	2.07	3.25	2.74	0.09	3.19	100.12	654	35	25	12	6	14	18	70	15.7	264	7.0	97	16	115
HS-48	mst	66.24	0.62	13.98	6.41	0.07	2.79	0.88	1.02	3.76	0.08	4.16	100.01	478	38	63	21	8	27	20	161	15.1	188	9.6	138	19	118
HS-49	mst	71.41	0.56	12.44	5.26	0.06	1.98	0.86	1.36	3.00	0.07	3.09	100.11	496	40	50	17	7	22	15	121	13.4	137	8.5	108	16	106
HS-50	mst	64.85	0.70	14.91	6.76	0.07	2.69	0.89	0.97	3.93	0.11	4.11	99.99	455	51	70	24	9	33	18	180	13.3	130	11.4	143	24	131
HS-51	vf sst	29.39	0.57	10.17	4.69	0.46	1.49	28.74	2.30	1.40	0.12	20.68	100.01	403	31	9	9	3	4	4	21	13.2	317	3.4	100	22	64
HS-52	mst	65.98	0.71	14.75	6.42	0.07	2.49	0.89	0.91	4.04	0.10	3.69	100.04	438	42	80	23	10	31	30	179	17.6	70	10.6	139	21	133
HS-53	vc sst	62.41	0.74	14.81	7.12	0.10	2.81	3.42	3.75	0.83	0.15	4.34	100.48	173	34	15	16	4	3	12	13	22.9	143	3.7	152	23	119
HS-54	f sst	60.24	0.68	15.20	6.90	0.12	2.68	4.75	3.74	0.58	0.11	5.21	100.20	64	24	12	18	4	5	14	5	24.8	139	2.8	150	19	101
HS-55	f sst	59.40	0.63	16.72	6.83	0.09	2.93	3.22	3.86	1.90	0.12	4.67	100.36	225	28	9	17	4	5	12	31	19.9	222	3.3	116	22	115
HS-56	mst	66.66	0.56	13.19	6.49	0.07	2.56	1.88	1.40	2.63	0.48	3.90	99.83	274	66	34	19	7	16	8	105	19.4	111	6.3	143	55	117
HS-57	m sst	59.88	0.84	16.07	7.82	0.13	3.16	3.32	4.22	1.63	0.15	3.18	100.39	361	33	19	17	5	6	12	37	25.2	261	3.5	196	23	121
HS-58	zst	71.21	0.51	12.34	5.13	0.05	1.88	1.30	1.39	2.67	0.08	3.37	99.94	301	31	40	16	5	16	17	105	14.8	98	6.3	128	17	102

Omori mudstone analyzed differ from the Kawai-Kuri Formation, with a broadly linear trend from mild depletion relative to UCC at the left to mildly enriched at the right (Fig. 4B). This trend is similar to that of average Cenozoic greywacke, although less regular. The patterns are similar to the range of Omori dacites from the Lake Jinzai (Izumo) area (Roser *et al.,* 2001), except for slight enrichment in MgO, and markedly greater Ni and Cr. The pattern for the two andesites analyzed here is almost a perfect match for the sandstones, supporting derivation of the sandstones from the underlying Omori volcanics.

Patterns for Fujina sandstones and mudrocks are almost flat and virtually identical (Fig. 4C). The lack of contrast between the two lithotypes reflects the very fine-grained nature of the sandstones. Abundances of most elements are very close to UCC levels, with the most notable deviations being depletion in Nb, CaO, Na_2O, and Sr. Most elements also lie within the range of compositions of San'in granitoids, suggesting that they were the main source for the Fujina sediments.

Average Ushikiri sandstones from west and east Shimane Peninsula have almost identical patterns, which overall are almost linear and slightly inclined from left to right (Fig. 5A). The sandstone averages compare quite well with the range of Omori dacites, but tend to lie at the upper edge of the range for Nb through to Sc, and to be less depleted for Ni and Cr. The patterns are thus a better match with average Omori andesite (Fig. 4B), and reflect the high proportion of andesitic detritus observed in Ushikiri sandstones. The patterns for average mudstones from west and east are also almost identical to each other. They differ from the sandstones only in relative depletion in CaO, Na_2O and Sr, and slight enrichment in K_2O, Rb, Ni, and Cr (Fig. 5A). Depletion of the former group is most likely due to destruction of plagioclase during source weathering. The enrichments seen in the latter group probably reflect higher abundances of clay minerals in the mud rocks, and hence are a product of limited sorting during turbidite deposition.

Comparison of the Ushikiri data with the Omori sandstones analyzed in this study shows the sandstone

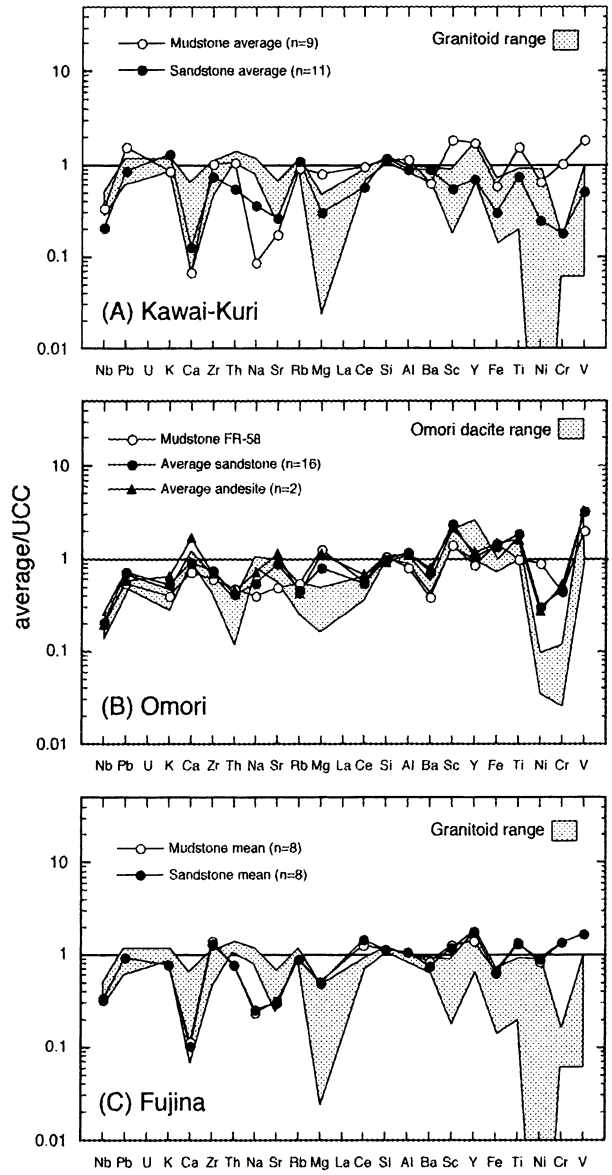

Fig. 4. UCC-normalized multi-element plots for average sandstones, mudrocks, and andesites (anhydrous normalized basis) from the Shinji-Matsue area: (A) Kawai-Kuri Formation, (B) Omori Formation; (C) Fujina Formation. Data from Table 1, excluding samples with >10% CaO to reduce dilution effects from authigenic or biogenic carbonate. Shaded zone on A and C is the compositional range (± one standard deviation from the mean) in San'in granitoids (S. Iizumi, unpubl. data compilation; n = 62 for major elements); shaded zone on B is the range in six Omori dacites from the Lake Fujina area (Roser *et al.*, 2001).

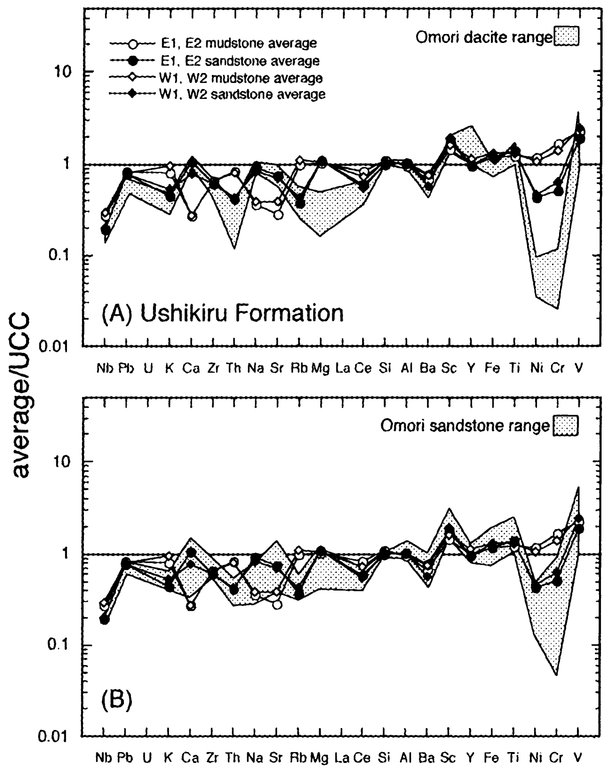

Fig. 5. UCC-normalized multi-element plots for average Ushikiri Formation sandstones and mudrocks (anhydrous normalized basis) from west Shimane Peninsula (W1 - Nagaohana; W2 - Uppurui) and east (E1 - Chikumi; E2 - Susumi). Data from Table 2, excluding samples with >10% CaO. (A) comparison with the compositional range (shaded) in six Omori dacites from the Lake Fujina area (Roser *et al.,* 2001); (B) comparison with the range (± one standard deviation) in Omori sandstones from the Shinji area (this study).

averages fall within the Omori range for all elements (Fig. 5B). The mudstone averages also compare well, with only small anomalies observed for CaO, Th, Sr, Rb, Ni, and Cr. The geochemical similarity between the Ushikiri and Omori Formations thus supports the correlation and facies relationships of these two units.

The chemical contrasts between the formations examined here are well illustrated by the Th/Sc-Zr/Sc plot of McLennan *et al.* (1993). The elements involved have low residence times in natural waters, and hence are transferred quantitatively from source to sediment (Taylor and McLennan, 1985). Both ratios increase from mafic to felsic volcanic rocks (Fig. 6A), and thus can be used as provenance indicators in first-cycle sediments. Kawai-Kuri sandstones and mudrocks have comparatively high Th/Sc and Zr/Sc ratios (Fig. 6A). The data trend across a model source evolution line, intersecting it near the position of average rhyolite and San'in granite. This trend is typical of sediments derived from felsic plutonic rocks, and represents a sorting effect, coupled with preferential concentration of zircons in coarser size grades. Fujina Formation samples also trend across the model source line, but at lower Th/Sc ratio and with much smaller range in Zr/Sc. This suggests the Fujina source was less felsic overall; the smaller range in Zr/Sc reflects the restricted grain size range in the sediments.

Omori sandstones have much lower values for both ratios, and plot in a cluster around the composition of Omori andesite and dacite (Fig. 6A). Their trend along the model evolution line is typical of volcaniclastic sediments in which both ratios may vary according to the proportion

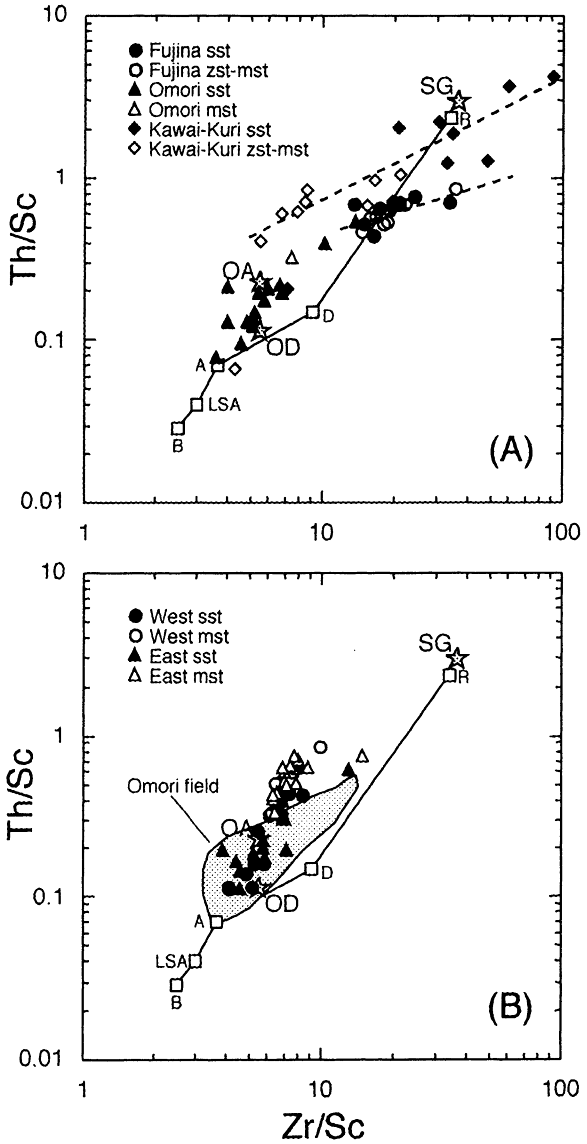

Fig. 6. Th/Sc-Zr/Sc plots (McLennan *et al.,* 1993) for the sandstones and mudrocks analyzed in this study: (A) Kawai-Kuri, Omori, and Fujina Formations; (B) Ushikiri Formation. Stars SG (San'in Granitoid; S. Iizumi data compilation), OA (Omori Andesite; this study), and OD (Omori Dacite; Roser *et al.,* 2001) are average ratios in potential source rocks. Lithotype abbreviations: sst - sandstone; zst - siltstone; mst - mudstone. Dashed lines on (A) illustrate sorting/heavy mineral concentration trends in the Kawai-Kuri and Fujina Formations; shaded field on (B) is the distribution of Omori sandstones from (A). Squares are volcanic rock averages: B - basalt; LSA - low-silica andesite; A - andesite; D - dacite; R - rhyolite; data after Taylor (1965, 1969). Solid line linking these averages defines a model source evolution line for first cycle volcanogenic sediments.

of differing lithic clasts. Ushikiri sandstones fall within the field defined by Omori equivalent, confirming the link between them (Fig. 6B). Ushikiri mudrocks have slightly higher values for both ratios, and define an overall trend that lies parallel to the model evolution line. This may be due to accumulation of felsic volcanic glass fragments in the finer size grades by virtue of their longer residence on the sea floor.

The results overall suggest that the Kawai-Kuri sediments were derived mainly from the Paleogene granitoids which crop out to the south in the Chugoku mountains. Overlying terrestrial and shallow marine Omori sediments were mainly derived from the andesitic to dacitic Omori volcanics with which they are intercalated or overlie. Deeper water correlatives in the Ushikiri Formation were also derived from the same source, and exhibit only slight contrasts in chemistry arising from turbidite deposition. Return to more felsic compositions in the Fujina Formation suggests derivation mainly from granitoids which were re-exposed following stripping of Omori volcanic cover. Lower Th/Sc and Zr/Sc ratios than in the arkosic Kawai-Kuri Formation suggests that the source was somewhat less felsic overall, possibly due to partial contribution from the Omori Formation. These changes illustrate the complexity which can be produced in proximal backarc sediments by dissection, volcanism, and renewed dissection at an active margin. A more detailed interpretation of the data will be given in future work.

Conclusions

Sandstones and mudrocks from the Kawai-Kuri Formation are silica-rich, and have elemental abundances and immobile element ratios compatible with derivation from Paleogene granitoids exposed to the south. Overlying Omori Formation sandstones have far more basic compositions, reflecting derivation from coeval andesites and dacites. These chemical fingerprints are also retained in deeper-water equivalents in the Ushikiri Formation of Shimane Peninsula, supporting their correlation. Return to more felsic compositions in the Fujina Formation implies renewed exposure of granitoid source rocks, coupled with contribution of more mafic detritus from remnants of Omori volcanics and sediments.

Acknowledgements

Our thanks to Yoshihiro Sawada for the use of the XRF, and to Mr. Y. Nagai (Kimachi Stone museum) for his help in accessing the Katsube Sekizaiten quarry. This work was supported by Monbukagakusho grant-in-aid 13440147 (B.P. Roser).

References

Blow, W. H., 1969, Late Middle Eocene to Recent planktonic foraminiferal biostratigraphy. *In:* Bronniman, P. and Renz, H. H. (eds), Intern. Conf. Planktonic Microfossils, 1st, Geneva (1967), Proc., **1**, 199-422.

Condie, K.C., 1993, Chemical composition and evolution of the upper continental crust: contrasting results from surface samples and shales. *Chem. Geol.,* **104**, 1-37.

Dinelli, E., Lucchini, F., Mordenti, A. and Paganelli, L., 1999, Geochemistry of Oligocene-Miocene sandstones of the northern

Apennines (Italy) and evolution of chemical features in relation to provenance changes. *Sed. Geol.*, **127**, 193-207.

Editorial Board of Geological Map of Shimane Prefecture (EBGMSP), 1997, Geological map of Shimane Prefecture (1:200,000).

Fujii, R., 2003, Geochemical provenance signatures in Miocene sedimentary rocks, Shinji-Tamatsukuri-Matsue. Unpubl. graduation thesis, Dept. of Geoscience, Shimane University, 77 p. +appendix.

Hashimoto, S., 2003, Geochemical comparison of Ushikiri Formation turbidites, east and west Shimane Peninsula. Unpubl. graduation thesis, Dept. of Geoscience, Shimane University, 76 p. +appendix.

Kano, K. and Takeuchi, K., 1989, Origin of mudstone clasts in turbidites of the Miocene Ushikiri Formation, Shimane Peninsula, Southwest Japan. *Sed. Geol.*, **62**, 79-87.

Kano, K., Takeuchi, K., Oshima, K. and Bunno, M., 1989, *Geology of the Taisha district. With geological sheet map at a scale of 1:50,000*. Tsukuba, Geological Survey of Japan, 58 p.*

Kano, K., Takeuchi, K. and Matsuura, H., 1991, *Geology of the Imaichi district. With geological sheet map at a scale of 1:50,000*. Tsukuba, Geological Survey of Japan, 79 p.*

Kano, K., Yamauchi, S., Takayasu, K., Matsuura, H. and Bunno, M., 1994, *Geology of the Matsue district. With geological sheet map at a scale of 1: 50,000*. Tsukuba, Geological Survey of Japan, 126 p.*

Kano, K., Matsuura, H., Sawada, Y. and Takeuchi , K., 1998, *Geology of the Iwami- Oda and Oura district. With Geological Sheet Map at 1: 50000*. Tsukuba, Geological Survey of Japan, 118 p.*

Kimura, J.-I. and Yamada, Y., 1996, Evaluation of major and trace element analyses using a flux to sample ratio of two to one glass beads. *Jour. Mineral. Petrol. Econ. Geol.*, **91**, 62-72.

McLennan, S.M., Hemming, S., McDaniel, D.K. and Hanson, G.N., 1993, Geochemical approaches to sedimentation, provenance and tectonics. *Geol. Soc. Amer. Spec. Pap.*, **284**, 21-40.

Morris P. A., Itaya, T., Watanabe, T. and Yamauchi, S., 1990, Potassium/argon ages of Cenozoic igneous rocks from eastern Shimane Prefecture-Oki Dozen Island, southwest Japan and the Japan sea Opening. *Jour. SW Asian Earth Sci.*, **4**, 125-131.

Ogasawara, K. and Nomura, R., 1980. Molluscan fossils from the Fujina Formation, Shimane Prefecture. *Mem. Volume for Prof. Saburo Kanno*, 79-98.

Roser, B.P., Sawada, Y. and Kabeto, K., 1998, Crushing performance and contamination trials of a tungsten carbide ring mill compared to agate grinding. *Geosci. Rep Shimane Univ.*, **17**, 1-11.

Roser, B.P., Kimura, J.-I. and Hisatomi, K. 2000. Whole-rock elemental abundances in sandstones and mudrocks from the Tanabe Group, Kii Peninsula, Japan. . *Geosci. Rep Shimane Univ.*, **19**, 101-112.

Roser, B.P., Tateishi, Y. and Nakayama, K., 2001, Whole-rock geochemical compositions of Miocene sedimentary and volcanic rocks from the Izumo -Matsue districts and Shimane Peninsula, SW Japan. *Geosci. Rep Shimane Univ.*, **20**, 69-82.

Sawada, Y., 2000, "Kimachi stone" as seen under the microscope. *Studies on Kimachi Stone*, **2**, 15-42.

Takayasu, K., Yamazaki, H., Ueda, T., Akagi, S., Matsumoto, T., Nomura, R., Okada, S., Sawada, Y., Yamauchi, S. and Yoshitani, A., 1992, Miocene stratigraphy and paleogeography of the San'in district, Southwest Japan. *Mem. Geol. Soc. Japan*, **37**, 97-116*.

Taylor, S.R., 1965, The application of trace element data to problems in petrology. In *Physics and Chemistry of the Earth*, vol. 6. (eds L.H. Ahrens, F. Press, S.K. Runcorn and H.C. Urey), Pergamon ,Oxford, pp. 133-213.

Taylor, S.R., 1969, Trace element chemistry of andesites and associated calc -alkaline rocks. In A.R. McBirney (ed.) *Proceedings of the Andesite Conference, 1969*, Department of Geology & Mineral Industries, Oregon, pp. 43-63.

Taylor, S.R. and McLennan, S.M., 1985, *The continental crust: its composition and evolution.* Blackwell Scientific Publications, Oxford, 312 p.

(Received: Oct. 14, 2004, Accepted: Nov. 28, 2004)

（要　旨）

B.P. Roser・藤井理恵・橋本真治，2004，宍道－松江地域並びに島根半島の中新統の主成分および微量成分元素分析．島根大学地球資源環境学研究報告，23，39-48

島根県の背弧海盆堆積物の地球化学データベースを増やす目的で，川合－久利層，大森層，牛切層，布志名層の堆積岩の主成分，微量成分元素分析を行った．サンプルは宍道－松江地域，並びに島根半島から収集した．川合－久利層の砂岩，泥岩はシリカに富み，ほとんどの元素は上部大陸地殻の組成(UCC)に対して枯渇しており，このことは堆積岩がフェルシックな花崗岩類を起源としていることを示している．その上位に重なる大森層の火山岩起源の砂岩は SiO_2 の含有量が低く，他の元素は UCC に近い値を示した．このことは堆積岩がこの地層の堆積と同時に形成された大森安山岩，デーサイトを起源としていることを反映している．大森層に対比され，深海のタービダイトからなる牛切層はほぼ大森層のものと同じ化学組成を示す．布志名層の泥岩と極細粒の砂岩は中程度に SiO_2 に富み，UCC に似た組成，あるいは UCC よりも少ない組成を持つ．これと不可動性の元素の比から，この地層はフェルシックな花崗岩類と従属的な大森層の火山岩類と堆積岩類の混合したものであることを示している．こうした化学組成の変化から，まず花崗岩類の露出・侵食がおこり，その後に火山活動，その噴出物の侵食が起きたことがわかる．